



# Molybdenum Nanoparticles Alleviate MC903-Induced Atopic Dermatitis-Like Symptoms in Mice by Modulating the ROS-Mediated NF- $\kappa$ B and Nrf2 /HO-1 Signaling Pathways

Qin Xiao<sup>1,\*</sup>, Jing Guo<sup>1,\*</sup>, Yongzhou Lu<sup>1</sup>, Jin Gao<sup>1</sup>, Chuanlong Jia<sup>1</sup>, Minghuan Huang<sup>1</sup>, Weifang Chu<sup>1</sup>, Wei Yao<sup>1</sup>, Peng Ning<sup>2</sup>, Qiannan Xu<sup>1</sup>, Nan Xu<sup>1</sup>

<sup>1</sup>Department of Dermatology, Shanghai East Hospital, School of Medicine, Tongji University, Shanghai, People's Republic of China; <sup>2</sup>Institute for Regenerative Medicine, Institute for Translational Nanomedicine, Shanghai East Hospital, Tongji University, Shanghai, People's Republic of China

\*These authors contributed equally to this work

Correspondence: Qiannan Xu; Nan Xu, Department of Dermatology, Shanghai East Hospital, School of Medicine, Tongji University, No. 150 Jimo Road, Shanghai, People's Republic of China, Tel +86 38804518, Email [greatfuturedoctor@hotmail.com](mailto:greatfuturedoctor@hotmail.com); [xnhrb1320@sohu.com](mailto:xnhrb1320@sohu.com)

**Purpose:** Atopic dermatitis (AD) is a chronic inflammatory skin condition that can affect individuals of all ages. Recent research has shown that oxidative stress plays a crucial role in the development of AD. Therefore, inhibiting oxidative stress may be an effective therapeutic approach for AD. Nano-molybdenum is a promising material for use as an antioxidant. We aimed to evaluate the therapeutic effects and preliminary mechanisms of molybdenum nanoparticles (Mo NPs) by using a murine model of chemically induced AD-like disease.

**Methods:** HaCaT cells, a spontaneously immortalized human keratinocyte cell line, were stimulated by tumor necrosis factor- $\alpha$  /interferon- $\gamma$  after pre-treatment with Mo NPs. Reactive oxygen species levels, production of inflammatory factors, and activation of the nuclear factor kappa-B and the nuclear factor erythroid 2-related factor pathways were then evaluated. Mo NPs was topically applied to treat a murine model of AD-like disease induced by MC903, a vitamin D3 analog. Dermatitis scores, pruritus scores, transepidermal water loss and body weight were evaluated. AD-related inflammatory factors and chemokines were evaluated. Activation of the nuclear factor kappa-B and nuclear factor erythroid 2-related factor / heme oxygenase-1 pathways was assessed.

**Results:** Our data showed that the topical application of Mo NPs dispersion could significantly alleviate AD skin lesions and itching and promote skin barrier repair. Further mechanistic experiments revealed that Mo NPs could inhibit the excessive activation of the nuclear factor kappa-B pathway, promote the expression of nuclear factor erythroid 2-related factor and heme oxygenase-1 proteins, and suppress oxidative stress reactions. Additionally, they inhibited the expression of thymic stromal lymphopoietin, inflammatory factors, and chemokines, thereby alleviating skin inflammation.

**Conclusion:** Mo NPs present a promising alternative treatment option for patients with AD as they could address three pivotal mechanisms in the pathogenesis of AD concurrently.

**Keywords:** oxidative stress, skin barrier function, chemokines, antioxidants, pro-inflammatory factors

## Introduction

AD is a chronic and recurrent inflammatory disease that is characterized by relapsing eczematous lesions and intense itching. It is the most prevalent inflammatory skin disorder, with an incidence ranging from 15% to 20% among children and approximately 10% in adults.<sup>1</sup> The Global Burden of Disease study reveals that AD ranks 15th among the most common non-fatal diseases. In terms of disability-adjusted life years, AD has the highest disease burden among skin diseases.<sup>2</sup> The pathogenesis of AD remains incompletely elucidated; however, genetic and environmental factors, destruction of epidermal barrier function, microbial imbalance, immune dysregulation, and skin inflammation are all

believed to play crucial roles. Moreover, these factors can mutually drive and enhance each other. For instance, a reduction in filaggrin (FLG) can lead to compromised skin barrier function that can exacerbate the aggregation of inflammatory and immune cells. Changes in skin barrier function that involve the malfunction of barrier-related proteins such as FLG and alterations in the intercorneocyte lipid composition, not only contribute to the typical skin dryness seen in patients with AD but also facilitate the increased penetration of allergens and pathogens.<sup>3</sup> This microenvironment notably contributes to the activation of Th2-mediated reactions and the release of proinflammatory cytokines including tumor necrosis factor-alpha (TNF- $\alpha$ ) and interleukins (IL-4, IL-13, IL-22).<sup>4,5</sup> Cytokines such as thymic stromal lymphopoietin (TSLP), IL-25, and IL-33, derived from the epithelium, contribute to the inflammatory state of the skin and initiate a Th2-mediated response in AD.<sup>6–8</sup> Oxidative stress is involved in many inflammatory skin diseases, such as psoriasis and vitiligo.<sup>9</sup> Recently, it has been suggested that excessive oxidative stress may be associated with the onset of AD.<sup>10</sup> Oxidative stress can cause direct damage to the cell membrane and DNA, impairing the epidermal skin barrier. Additionally, oxidative stress activation stimulates the nuclear factor kappa-B (NF- $\kappa$ B) pathway that induces the release of inflammatory factors such as IL-6, IL-8, IL-9, and IL-33. The skin barrier dysfunction triggers an inflammatory response in the dermis, further promoting the release of inflammatory factors. The inflammatory response of the skin can also trigger the production of reactive oxygen species (ROS), thus forming a self-sustaining vicious circle.<sup>11</sup> Hence, mitigating the oxidative stress induced by ROS in AD lesions may play a crucial role in improving dermatitis in individuals with AD.

Molybdenum is a trace element that is important for many physiological processes and human survival.<sup>12</sup> It is found in most foods and is part of a complex called molybdenum cofactor that is required for three mammalian enzymes: xanthine oxidase, aldehyde oxidase, and sulfite oxidase.<sup>13</sup> The total body content of Molybdenum is less than 9 mg and most organs and tissues contain trace amounts of it.<sup>14</sup> Nanomaterials and nanocarriers with favorable rheological properties and stability have shown significant potential in repairing skin damage.<sup>15,16</sup> Previous studies have demonstrated that nanoparticles have an enhanced capability to penetrate the skin and target lesion areas, making them promising for the treatment and management of skin conditions.<sup>17,18</sup> Molybdenum-based nanoparticles are a class of transition metal nanomaterials that exhibit unique physical and chemical properties. These properties include large surface area, easy surface modification, and efficient near-infrared photothermal energy transfer capabilities.<sup>19</sup> Nano-molybdenum is a promising material for use as an antioxidant. Our previous research has confirmed that nano-molybdenum exhibits strong antioxidant capability *in vitro*. Animal experiments have further validated that nano-molybdenum materials can promote wound healing and stimulate hair growth by inhibiting oxidative stress reactions.<sup>20,21</sup> Previous studies have indicated that Mo disulfide (MoS<sub>2</sub>)-based nanocomposites exhibited a substantial antioxidant effect in cancer therapy.<sup>22,23</sup> A recent article by Zhang et al suggested that zero-valent molybdenum nanodots could down-regulate the amount of ROS and reduce colitis in a mouse model of inflammatory bowel disease without significant side effects.<sup>24</sup> It was confirmed that MoO<sub>3</sub> particles of different sizes and morphologies had good antimicrobial activity and were able to completely destroy *Staphylococcus epidermidis* ATCC 12228 strain.<sup>25,26</sup> Studies have found *Staphylococcus* species expand during AD flares. Antimicrobials are common treatments and can reduce both staphylococcal relative abundances and disease severity.<sup>27</sup> Based on this, we hypothesized that Mo NPs could alleviate skin lesions in AD by inhibiting oxidative stress in the skin. To assess the impact of Mo NPs on AD inflammation, 15–30 nm diameter Mo NPs were synthesized, dissolved in deionized water (DI), and prepared as a dispersion. The topical application of Mo NPs dispersion significantly improved the severity of AD skin lesions, alleviated the intense itching associated with AD, and restored the impaired skin barrier function. Moreover, it mitigated the weight loss observed in AD mice. To further explore the mechanisms underlying the amelioration of AD skin lesions by Mo NPs, oxidative stress-related signaling pathways, including the NF- $\kappa$ B and nuclear factor erythroid 2-related factor (Nrf2)/heme oxygenase-1(HO-1) signaling pathways, were investigated. The results confirmed that the use of Mo NPs dispersion ameliorated skin lesions by inhibiting the NF- $\kappa$ B pathway, promoting the Nrf2/HO-1 signaling pathway, and suppressing oxidative stress reactions in the skin. These discoveries indicated that Mo NPs dispersion possessed excellent ROS scavenging ability and presented an effective approach for treating AD.

## Materials and Methods

### Materials and Reagents

Mo powder and isopropanol were purchased from Macklin (Shanghai, China).  $H_2O_2$  was obtained from Yukacell (Shanghai, China). Hydrogen peroxide detection reagent was obtained from LOHAND (Hangzhou, China). HaCaT cells were purchased from Fuheng Biology (Deyang, China). Phosphate-buffered saline (PBS), Dulbecco's modified Eagle's medium (DMEM), fetal bovine serum (FBS), streptomycin and penicillin were obtained from Gibco (Waltham, MA, USA). A CCK-8 assay kit was purchased from Yeasen (Shanghai, China). Recombinant TNF- $\alpha$  and IFN- $\gamma$  proteins were obtained from Peptotech (Rocky Hill, USA). Enzyme-linked immunosorbent assay (ELISA) kits were obtained from Nanjing Jiancheng Bioengineering Institute (Nanjing, China). A ROS assay kit was obtained from Beyotime (Shanghai, China). TRIzol was obtained from Invitrogen (California, USA). The cDNA synthesis kit and SYBR Green fluorescence master mix were obtained from TaKaRa (Beijing, China). Radioimmunoprecipitation assay lysis buffer and the bicinchoninic acid protein detection kit were purchased from Beyotime (Shanghai, China).

### Synthesis and Characterization of Mo NPs

Mo NPs were synthesized as described previously through the mechanical exfoliation of a blend comprising 6 g Mo powder and 100 mL isopropanol for 20 h at 450 W with a 75% duty cycle.<sup>20,21</sup> Mechanical exfoliation was carried out by an ultrasonic disrupter (Fisher Scientific™ Model 120, Pittsburgh, USA). The supernatant was collected, and the isopropanol was removed using a rotary evaporator. The prepared Mo NPs were dispersed and dissolved in DI. The transmission electron microscopy (TEM) electron micrographs were acquired using the FEI Tecnai F30 Microscope (Eindhoven, The Netherlands). The hydrodynamic particle size and zeta potential of different Mo NPs were analyzed in distilled water using Dynamic light scattering (Zeta SIZER NANO ZS90, Malvern Ltd, Malvern, United Kingdom), while the X-ray photoelectron spectroscopy (XPS) spectra were collected using the Thermo Scientific K-Alpha instrument (Waltham, MA, USA). In order to evaluate their antioxidant capacity, Mo NPs were co-reacted with  $H_2O_2$  (0.1 mM) at different concentrations (0, 40, 80, 120, 160, 300 and 320 ppm). After incubating for three minutes, the residual concentration of  $H_2O_2$  was measured using a hydrogen peroxide detection reagent.

### Cell Culture and CCK8 Assay

HaCaT cells that are adherent cells were used in this study. HaCaT cells were cultured in DMEM comprising 10% (v/v) FBS and antibiotics (100 U/mL penicillin and 100  $\mu$ g/mL streptomycin) at 37°C in a humidified 5%  $CO_2$  incubator. Cells from the third passage were used for the experiments. Cell viability was measured by the CCK-8 kit assay. HaCaT cells were seeded in 96-well plates at the density of  $5 \times 10^3$  cells per well, stabilized for 24 h, replaced with a serum-free medium containing varying concentrations of Mo NPs (0, 3.75, 37.5, 75, 150, 300, 600, 900, and 1200 ppm), and incubated for 24 h, 48 h, and 72 h. Then, CCK-8 solution was added, and the cells were further incubated for 2 h away from light. Following incubation, absorbance was detected at 450 nm by a spectrophotometer (Thermo Fisher Scientific, Waltham, MA, USA). Results were expressed as a percentage of cell viability.

### Reactive Oxygen Species Assay

The ROS assay was performed using the ROS assay kit in strict accordance with instructions. HaCaT cells ( $2 \times 10^5$  cells/well) were cultured in a 24-well plate for 24 h. In the TNF- $\alpha$ /IFN- $\gamma$  stimulated group, HaCaT cells were treated with TNF- $\alpha$ /IFN- $\gamma$  (10 ng/mL each) with or without Mo NPs (300 ppm) for 24 h, and the ROS assay was performed. In cellular oxidative stress mode, cells were treated with or without Mo NPs dispersion for 24 h and then incubated with  $H_2O_2$  (0.1 mM) for 0.5 h in the dark. The supernatant was removed, and the cells were washed with PBS twice. Intracellular ROS was quantified with 2,7-dichlorodihydrofluorescein diacetate (DCFH-DA). DCFH-DA was loaded into the cells as a fluorescent probe. Cells were incubated in serum-free culture medium containing DCFH-DA at a concentration of 10  $\mu$ mol/L for 30 minutes in the dark. Subsequently, cells were washed three times with PBS to thoroughly remove the probe that had not entered the cells. The results were observed under an inverted fluorescence

microscope with a 488 nm excitation wavelength. Fluorescent micrographs were acquired using a fluorescence microscope Zeiss Axio Vert.A1 (Oberkochen, Germany).

## Enzyme-Linked Immunosorbent Assay

HaCaT cells ( $5 \times 10^6$  cells/well) were cultured with TNF- $\alpha$ /IFN- $\gamma$  (all 10 ng/mL) in the presence or absence of Mo NPs (300 ppm) for 24 h in a 6-well plate. The supernatant of the HaCaT cell culture medium was harvested, and the cytokine (IL-4, IL-13, IL-33 and TSLP) concentrations were measured by ELISA kits by following the instructions of the manufacturer. The absorbance was measured at 450 nm by a microplate reader.

## Animals

The Institutional Animal Care and Use Committee of the Experimental Animal Welfare and Ethics Management Committee of Tongji University (Laboratory animal licences 2020–002, Shanghai, China) approved all animal experiments. Six-week-old male C57BL/6 mice (obtained from JSJ Experimental Animal Company, Shanghai, China) were housed under specific pathogen-free conditions ( $24 \pm 2$  °C, 12 h/12 h light/dark cycles, 45–55% humidity) and were given free access to standard chow and water. Mice were raised for 1 week to acclimate to the environment. Subsequently, all mice were randomly divided into three groups of three mice each: (1) control group; (2) MC903 group; (3) Mo group. The control group received no treatment. The MC903 group received a daily treatment of 0.1 mL MC903 (0.1 mM) on their dorsal skin for 12 days. The Mo group was administered with both 0.1 mL MC903 (0.1 mM) and 0.1 mL Mo NPs dispersion (300 ppm) daily on their backs for 12 days. Mo NPs was performed 1 h after the MC903 challenge. After applying the treatment to the mouse skin, the surface droplets disappeared within 10 minutes under anesthesia. Prior to the experiment, an approximately 2 cm  $\times$  3 cm area of fur on the back of the mouse was removed using an electric shaver. The remaining hairs in the shaved area were then removed with depilatory cream. On day 13, mice were sacrificed by cervical neck dislocation, and dorsal skin samples were collected for further examination.

## Evaluation of Dermatitis Scores, Pruritus Scores, Transepidermal Water Loss and Body Weight

The severity of dermatitis in the dorsal skin was assessed macroscopically on day 0, 2, 4, 6, and 8. Dermatitis scores were assigned according to the following scoring procedure.<sup>28</sup> Mice were assessed and scored (ranging from 0 to 12) for erythema (redness, hemorrhage), edema (swelling), erosion (excoriation), and desquamation (scaling, crusting) on a scale from 0 to 3: 0 indicating no symptoms, 1 for mild symptoms, 2 for moderate symptoms, and 3 for severe symptoms. The overall severity score for dermatitis was calculated as the sum of individual scores. Pruritus is one of the major clinical manifestations in AD. To investigate AD-like behavioral changes, the frequencies of mice rubbing the dorsal skin with hind paws for a 10 min period immediately after administration was measured and recorded on day 4, and 8. Transepidermal water loss (TEWL) was measured by GPSkin Barrier (GPOWER Inc, Seoul, South Korea) and determined from three replicate measurements from each mouse on day 0, 2, 4, 6, 8, and 10. The body weight of each mouse was measured on day 1, 3, 5, 7, 9, and 11.

## Histopathological Analysis and Immunohistochemistry

Mouse dorsal skin samples were excised and fixed in 10% formalin overnight. The skin sections were dehydrated in graded ethanol, cleared in xylene, and embedded in paraffin. Then, the specimens were sectioned into 5  $\mu$ m-thick slices. The sections were stained with hematoxylin and eosin (H&E) to visualize epidermal thickness and assess histological changes. They were examined under a light microscope. Epidermal thickness was measured by Image J software. The immunohistochemistry (IHC) staining was performed as described previously.<sup>29</sup> Antibodies against iNOS (BA0362, Boster, 1:1000), COX2 (BA0738, Boster, 1:150), TSLP (ab47943, Abcam, 1:100) and TNF- $\alpha$  (Beyotime, AF8208, 1:100), were used as primary antibodies. The IHC stain analysis was performed using the Image J IHC Toolbox.

## Quantitative Reverse Transcriptase- Polymerase Chain Reaction (qRT-PCR)

Total RNA was extracted from HaCaT cells or dorsal skin tissue samples using TRIzol. For cDNA synthesis, total RNA was reverse transcribed using a cDNA synthesis kit. The polymerase chain reaction (PCR) primers were synthesized and the sequences of primers pairs were as follows: Human  $\beta$ -actin, forward 5' AAG GTG ACA GCA GTC GGT T 3', reversed 5' TGT GTG GAC TTG GGA GAG G 3'. Human FLG, forward 5' GAC AAT AGG AAG AGG CTA AGT 3', reversed 5' TGT GTA ATATGT GGC AATATG 3'. Human MDC, forward 5' AGA CAC CTG GGC TGA GAC ATA 3', reversed 5' CAG ACG GTA ACG GAC GTA ATC 3'. Human RANTES, forward 5' GTG CCC ACA TCA AGG AGT ATT 3', reversed 5' CCG AAC CCATTT CTT CTC TG 3'. Human TARC, forward 5' GCC ATC GTT TTT GTA ACT GT 3', reversed 5' GCATTC TTC ACT CTC TTG TTG T 3'. Mouse  $\beta$ -actin, forward 5' CCT CTA TGC CAA CAC AGT 3', reversed 5' AGC CAC CAA TCC ACA CAG 3'. Mouse IL-4, forward 5' ACG AAG AAC ACC ACA GAG AGT 3', reversed 5' GAA AAG CCC GAA AGA GTC T 3'. Mouse IL-13, forward 5' CAG CCT CCC CGA TAC CAA AAT 3', reversed 5' CCC CAG CAA AGT CTG ATG TGA 3'. Mouse TSLP, forward 5' GCT ACC CTG AAA CTG AGA GAA 3', reversed 5' TGA AGG AAT ACC ACA ATC TTA GAA 3'. Mouse MDC, forward 5' TAT CTG CTG CCA GGA CTA CAT 3', reversed 5' TCT CGG TTC TTG ACG GTT AT 3'. Mouse TARC, forward 5' GAG AGT GCT GCC TGG ATT ACT TC 3', reversed 5' CTT GCC CTG GAC AGT CAG A 3'. Mouse RANTES, forward 5' AGG ATA GAG GGT TTC TTG ATT C 3', reversed 5' GTG GGA GTA GGG GAT TAC TG 3'. Mouse FLG, forward 5' CAA AGA GAG GGA AAC AGA AGA 3', 3' CTG CCT CCT TCA GAG TCA C 5'. Real-time PCR was performed using a quantitative amplification system (ABI PRISM 7500 Fast Real-time PCR System; Applied Biosystems, Foster City, CA, USA) in a 20  $\mu$ L reaction volume, containing 10  $\mu$ L SYBR Green fluorescence master mix, 5  $\mu$ L primer, and 5  $\mu$ L quantified cDNA template. The relative expression level of target genes was determined using the  $2^{-\Delta\Delta C_t}$  method.

## Western Blotting

Mouse dorsal skin tissue samples were lysed in radioimmunoprecipitation assay lysis buffer, homogenized and centrifugated at 13,500 rpm for 15 min at 4°C to separate the supernatants. HaCaT cells ( $2 \times 10^6$  cells/well) were cultured with TNF- $\alpha$ /IFN- $\gamma$  in the presence or absence of Mo NPs (300 ppm) for 24 h. RIPA lysis buffer containing phenylmethylsulfonyl fluoride was used to extract total cellular protein, according to the instructions of the manufacturer. Protein concentration was determined using the bicinchoninic acid protein detection kit. Protein samples were directly loaded onto sodium dodecyl-sulfate polyacrylamide gel electrophoresis gel wells and electrophoresis buffer was added to initiate electrophoresis. After electrophoresis, the proteins were transferred to a polyvinylidene fluoride membrane. The PVDF membrane was then incubated with blocking solution (5% skim milk solution) at room temperature for 1 h. Following that, the membrane was incubated with primary antibodies at 4°C overnight. The membrane was washed three times using tris-buffered saline Tween-20 buffer, incubated with diluted horse-radish peroxidase-conjugated secondary antibody (Cat.# ab6721, Abcam) for 2 h at room temperature, and then washed three times with TBST buffer for 10 min each time. Finally, the PVDF membrane was incubated with the chemiluminescent substrate (Cat. # 5200, Tanon) and was detected with a full-function luminometer (Cat. # FR-1800, Furi technology).  $\beta$ -Actin was used as the internal standard, the relative expression was calculated, and the experiment was repeated three times. Primary antibodies included anti-Nrf2 (1:1000, Cat. # AF0639, Affinity), anti-p65 (1:1000, Cat. # 3033T, CST), anti-p-P65 (1:1000, Cat. # BF8005, Affinity), anti-HO-1 (1:1000, Cat. # BF8020, Affinity), and anti- $\beta$ -actin (1:2000, Cat. # 66009-1-Ig, Proteintech).

## Statistical Analysis

All statistical analyses were performed by using Prism 8.0 software (GraphPad Software). All experiments were repeated at least three times with duplicates and results were reported as mean $\pm$ SD (standard deviation). Significant differences among multiple groups were assessed by ANOVA with Tukey's multiple comparison test. Results were regarded statistically significant when the P-value was <0.05.

## Results

### Synthesis and Characterization of Mo NPs

Mo NPs were synthesized via mechanical exfoliation of Mo powder in isopropanol. Mo NPs were dissolved in DI. Figure 1a shows the overall appearance of the Mo NPs dispersion (300 ppm). TEM results confirmed that the Mo NPs

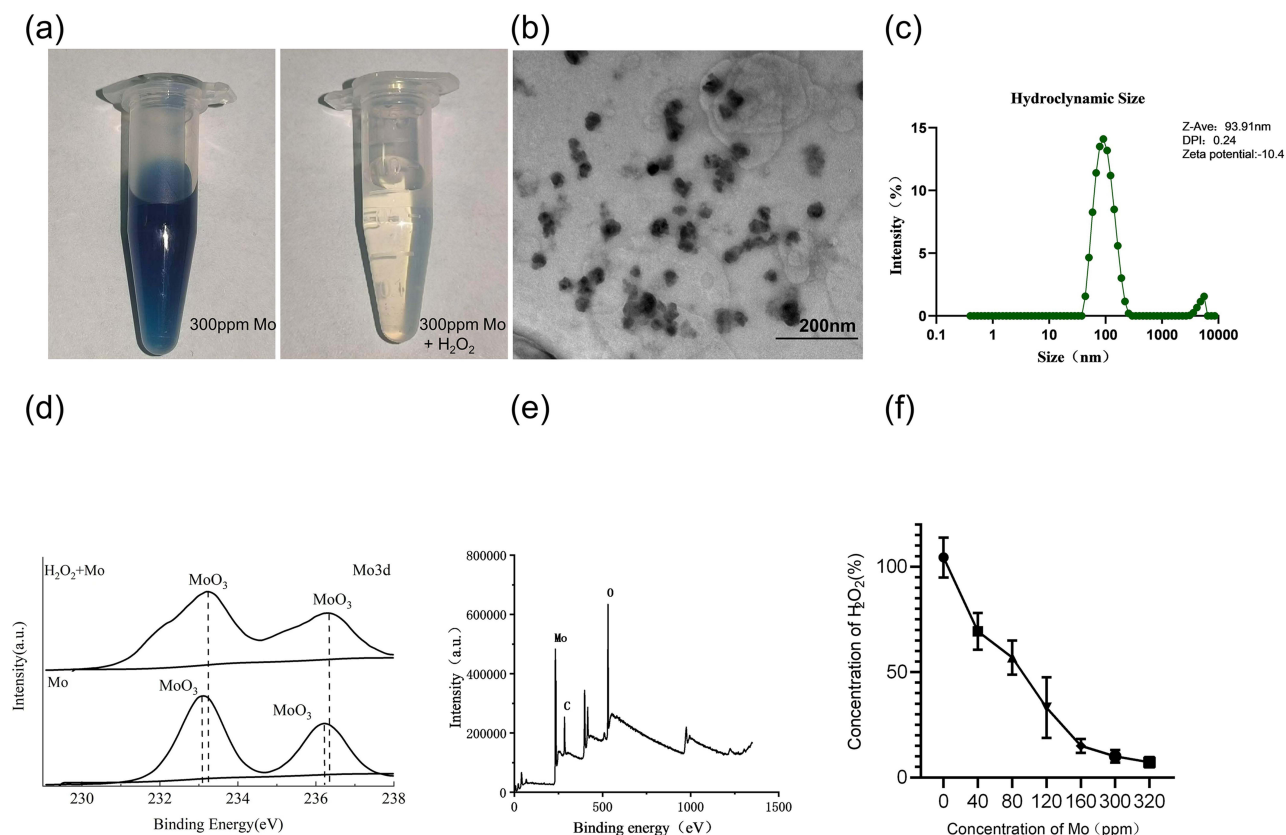


**Figure 1** Characterization of Mo NPs. (a) Photographs of Mo NPs (300 ppm) in deionized water (left) and in 0.1 mM H<sub>2</sub>O<sub>2</sub> (right). (b) TEM micrograph of Mo NPs. (c) Hydration particle sizes of Mo NPs. (d) XPS spectra of Mo 3d of Mo and oxide Mo. (e) XPS spectrum of Mo NPs. (f) Scavenging H<sub>2</sub>O<sub>2</sub> by Mo NPs at a range of concentrations (mean±SD, n = 3).

were uniform in size, evenly distributed, and had a diameter of 15–30 nm (Figure 1b). The hydration particle size distribution of Mo NPs was 93.91 nm and the zeta potential of Mo NPs was  $-10.4$  mV (Figure 1c). As shown in Figure 1d, the binding energy of the Mo 3d oxide increased by 0.2 eV after co-reacting with H<sub>2</sub>O<sub>2</sub> (0.1 mM). XPS revealed that Mo NPs contained Mo and O atoms (Figure 1e). To evaluate the antioxidant capacity of Mo NPs, Mo NP dispersion of different concentrations were co-reacted with H<sub>2</sub>O<sub>2</sub> (0.1mM). The result showed that Mo NPs could significantly downregulate the concentration of H<sub>2</sub>O<sub>2</sub>. As illustrated in Figure 1f, the H<sub>2</sub>O<sub>2</sub> scavenging rates of Mo NPs dispersion increased with higher Mo NP concentrations. At 300 ppm, the Mo NP dispersion exhibited an ability to scavenge nearly 90% of H<sub>2</sub>O<sub>2</sub>. The results showed that Mo NPs were successfully synthesized and had *in vitro* antioxidant properties for H<sub>2</sub>O<sub>2</sub> scavenging.

## Effects of Mo NPs on HaCaT Cell Viability and ROS Generation

To investigate the impact of Mo NP dispersion on HaCaT cell viability, cells were incubated with different concentrations of Mo NP dispersion. The cells were then harvested at 24 h, 48 h and 72 h for the CCK8 assay. We observed that Mo NPs did not affect cell viability at concentrations as high as 300 ppm but cell viability decreased at concentrations of 600 ppm (Figure 2a). However, the impact of Mo NPs dispersion on cell viability did not increase with increased exposure time. The results demonstrated that Mo NPs dispersion at a concentration of 300 ppm did not affect cell viability. Our data were consistent with previous findings.<sup>30</sup> Moreover, Mo NPs were observed to eliminate 90% of H<sub>2</sub>O<sub>2</sub> *in vitro*. Therefore, a 300 ppm dispersion of Mo NPs was used for subsequent cell culture and animal-based experiments. Studies have confirmed that ROS play an important role in the pathogenesis of AD.<sup>31</sup> To determine whether Mo NP dispersion could suppress ROS generation, HaCaT cells were cultured with H<sub>2</sub>O<sub>2</sub> for 0.5 h to create a cellular oxidative stress model. The fluorescence intensity of cells which were not pre-treated with Mo NPs, but only stimulated by H<sub>2</sub>O<sub>2</sub>

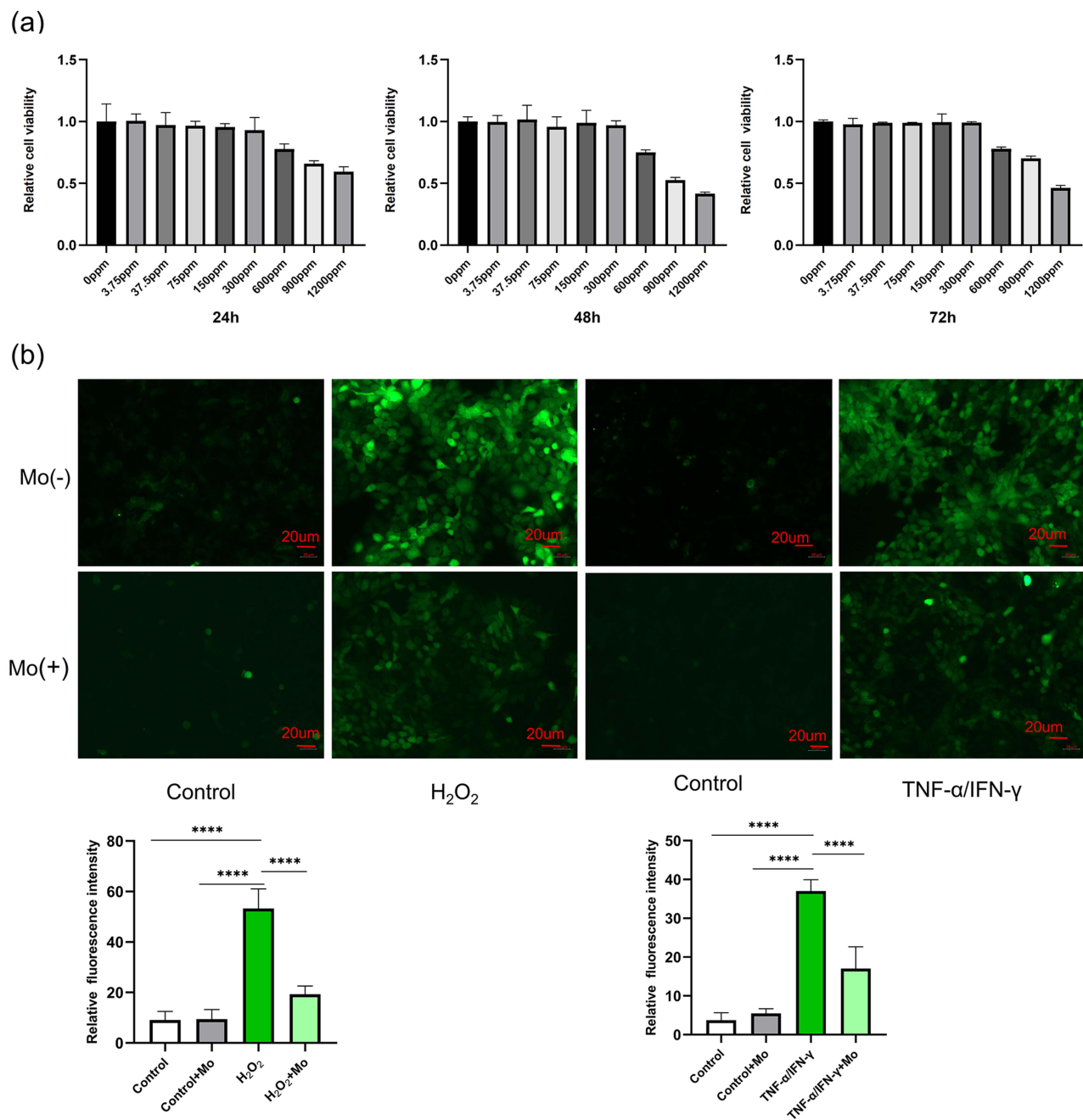


**Figure 2** Effect of Mo NPs on HaCaT Cells. (a) The impact of Mo NPs on HaCaT cell viability. (b) Mo NPs suppress ROS generation in HaCaT cells in various oxidative stress models. Data were represented as mean $\pm$ SD from three independent replicates, and P values were calculated by ANOVA with Tukey's honest significant difference *post-hoc* test (\*\*\*\*P < 0.0001).

was remarkably increased, and it was significantly reduced in a cellular oxidative stress model involving pre-treatment with Mo NPs dispersion (Figure 2b). These findings validated the ability of Mo NPs to efficiently reduce intracellular ROS. This was further verified in another model where cells were treated with TNF- $\alpha$ /IFN- $\gamma$ . HaCaT cells stimulated by TNF- $\alpha$ /IFN- $\gamma$  showed a significant increase in intracellular ROS levels (Figure 2b). When the TNF- $\alpha$ /IFN- $\gamma$ -treated cells were pre-treated with Mo NPs dispersion, the level of intracellular ROS was markedly reduced. These data indicated that Mo NPs dispersion can significantly reduce the generation of ROS in keratinocytes after stimulation with H<sub>2</sub>O<sub>2</sub> or TNF- $\alpha$ /IFN- $\gamma$ .

## Mo NPs Downregulated Expression of Pro-inflammatory Cytokines and Chemokines in TNF- $\alpha$ /IFN- $\gamma$ Stimulated HaCaT Cells

TNF- $\alpha$ /IFN- $\gamma$  can stimulate the expression of pro-inflammatory factors and chemokines such as IL-6, IL-8, CCL17, and CCL22.<sup>32</sup> Consequently, this treatment is widely utilized to stimulate HaCaT cells and construct in vitro models of AD.<sup>33,34</sup> The impact of Mo NPs dispersion on the secretion of Th2 cytokines and chemokines was evaluated using ELISA. As shown in Figure 3a, a 300 ppm Mo NPs dispersion significantly inhibited the expression of IL-4, IL-13, IL-33 and TSLP in TNF- $\alpha$  /IFN- $\gamma$  stimulated HaCaT cells.

Additionally, a qRT-PCR assay was employed to assess the influence of Mo NPs dispersion on the expression of mRNAs for macrophage-derived chemokines (MDC, CCL22), thymic and activating regulatory chemokines (TARC, CCL17), those secreted by activated T cells (RANTES, CCL5), and FLG in TNF- $\alpha$ /IFN- $\gamma$  induced HaCaT cells. The mRNA levels of MDC, TARC and RANTES were significantly inhibited by Mo NPs dispersion compared with those in the AD model group (Figure 3b). FLG is an important epidermal protein that plays a crucial role in the pathogenesis of allergic diseases such as AD. Impaired skin barrier function in patients with AD is often accompanied by a significant decrease in FLG expression.<sup>35</sup> The mRNA expression of the FLG locus in TNF- $\alpha$ /IFN- $\gamma$  stimulated HaCaT cells was significantly inhibited. However, Mo NPs dispersion treatment could significantly increase FLG expression (Figure 3b).

These results demonstrated that Mo NPs dispersion inhibited the expression of inflammatory factors IL-4, IL-13, IL-33, and TSLP in keratinocytes that play a crucial role in the pathogenesis of AD. Mo NPs dispersion also down-regulated the expression of the chemokines MDC, TARC and RANTES, but upregulated the expression of the skin barrier-related gene FLG.

## Mo NPs Suppressed the NF- $\kappa$ B Signaling Pathway and Promoted the Expression of Nrf2 and HO-1 in TNF- $\alpha$ /IFN- $\gamma$ Stimulated HaCaT Cells

It is widely recognized that NF- $\kappa$ B plays a crucial role in the production of pro-inflammatory cytokines and chemokines including MDC and TARC.<sup>36</sup> In order to further understand the molecular mechanism underlying the anti-inflammatory activity of Mo NPs dispersion in TNF- $\alpha$ /IFN- $\gamma$  stimulated HaCaT cells, the impact of Mo NPs dispersion on the activation of the NF- $\kappa$ B signaling pathway was investigated. The phosphorylation levels of NF- $\kappa$ B P65 protein were analyzed using Western blotting.

HaCaT cells triggered by TNF- $\alpha$ /IFN- $\gamma$  exhibited a significant increase in NF- $\kappa$ B P65 phosphorylation. Mo NPs dispersion markedly inhibited P65 phosphorylation compared to the TNF- $\alpha$ /IFN- $\gamma$  single treatment group (Figure 3c). These results indicated that Mo NPs suppressed overactivation of the NF- $\kappa$ B signaling pathway by inhibiting phosphorylation of NF- $\kappa$ B P65 protein. HO-1 is a gene regulated by Nrf2 and it plays an essential role in combating inflammation and oxidation and exerts cytoprotective effects. Previous studies have revealed that treating AD leads to elevated expression levels of HO-1 and Nrf2, suggesting an important role for HO-1 and Nrf2 in the therapeutic approach to AD.<sup>37,38</sup> The Nrf2/HO-1 pathway restricts skin inflammation by suppressing the production of inflammatory cytokines.<sup>39,40</sup> The influence of Mo NPs dispersion on the expression of the Nrf2/HO-1 pathway was investigated using Western blotting. The results showed that the expression of Nrf2 and HO-1 proteins in keratinocytes induced by TNF- $\alpha$ /IFN- $\gamma$  significantly was reduced; However, Mo NPs dispersion treatment could markedly enhance Nrf2/HO-1 expression (Figure 3c).

Based on these results, we hypothesized that TNF- $\alpha$ /IFN- $\gamma$  inhibited Nrf2 and HO-1 protein expression by promoting the overactivation of the NF- $\kappa$ B signaling pathway. Mo NPs have the potential to restrain the overactivation of the NF- $\kappa$ B signaling pathway, enhance the expression of Nrf2 and HO-1, decrease ROS production, and mitigate excessive oxidative stress in HaCaT cells.

## Mo NPs Ameliorated MC903-Induced AD-Like Symptoms and Recovered Skin Barrier Function

To investigate the effects of topically applied Mo NPs dispersion on AD-like lesions, a murine model of AD-like disease was established by topical use of MC903, an analog of vitamin D3. Figure 4a is a schematic diagram of the experimental



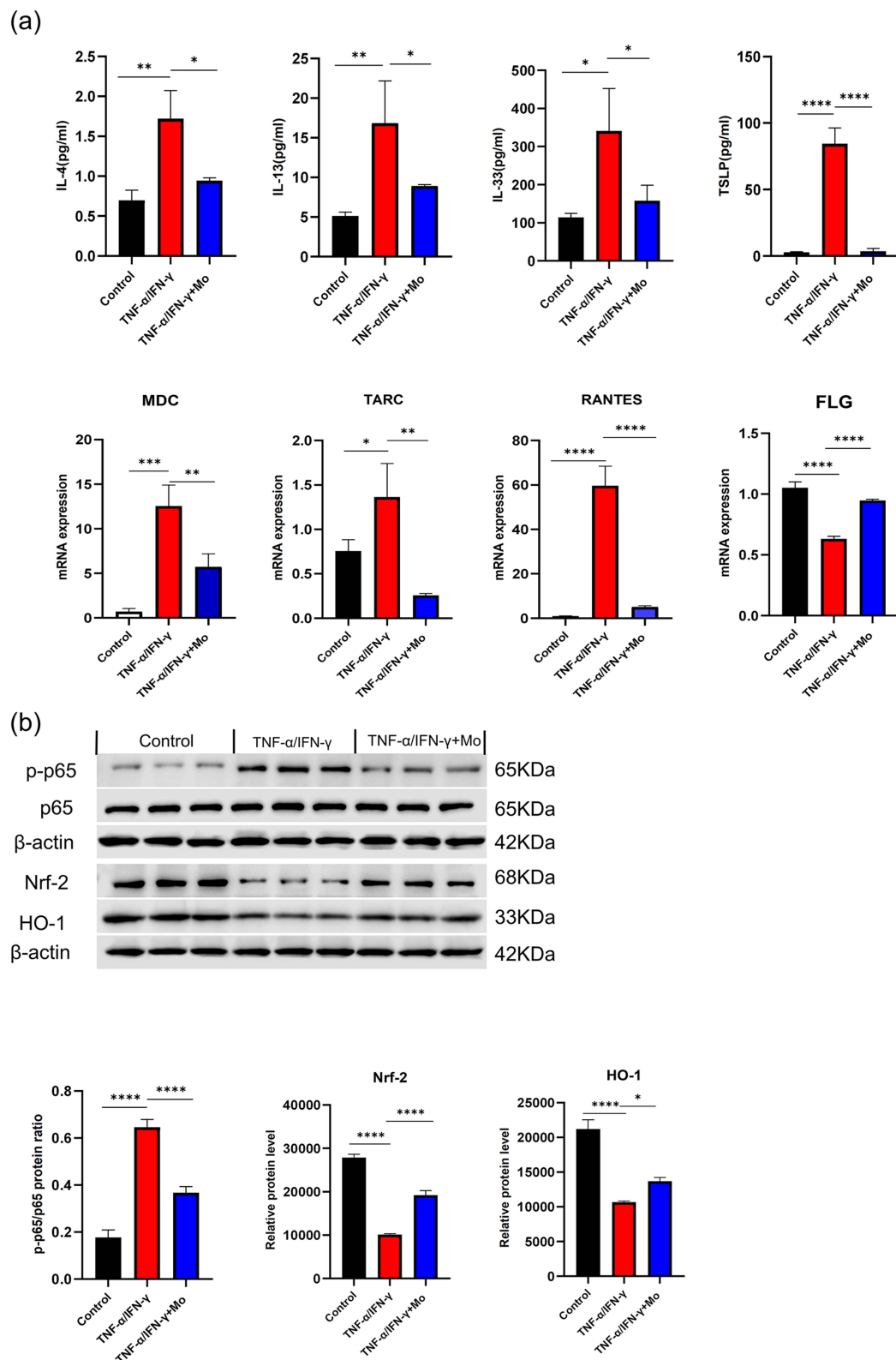


**Figure 3** The impact of Mo NPs on HaCaT cells. (a) The effect of Mo NPs on the expression of inflammatory factors (IL-4, IL-13, IL-33, TSLP), FLG and chemokine genes (MDC, TARC and RANTE) in TNF- $\alpha$ /IFN- $\gamma$ -stimulated HaCaT cells. (b) The effects of Mo NPs on the NF- $\kappa$ B signaling pathway and Nrf2/HO-1 pathway in TNF- $\alpha$ /IFN- $\gamma$  -stimulated HaCaT cells. Data were represented as mean $\pm$ SD from three independent replicates, and P values were calculated by ANOVA with Tukey's honest significant difference post-hoc test (\*P < 0.1, \*\*P < 0.01, \*\*\*P < 0.001, and \*\*\*\*P < 0.0001).

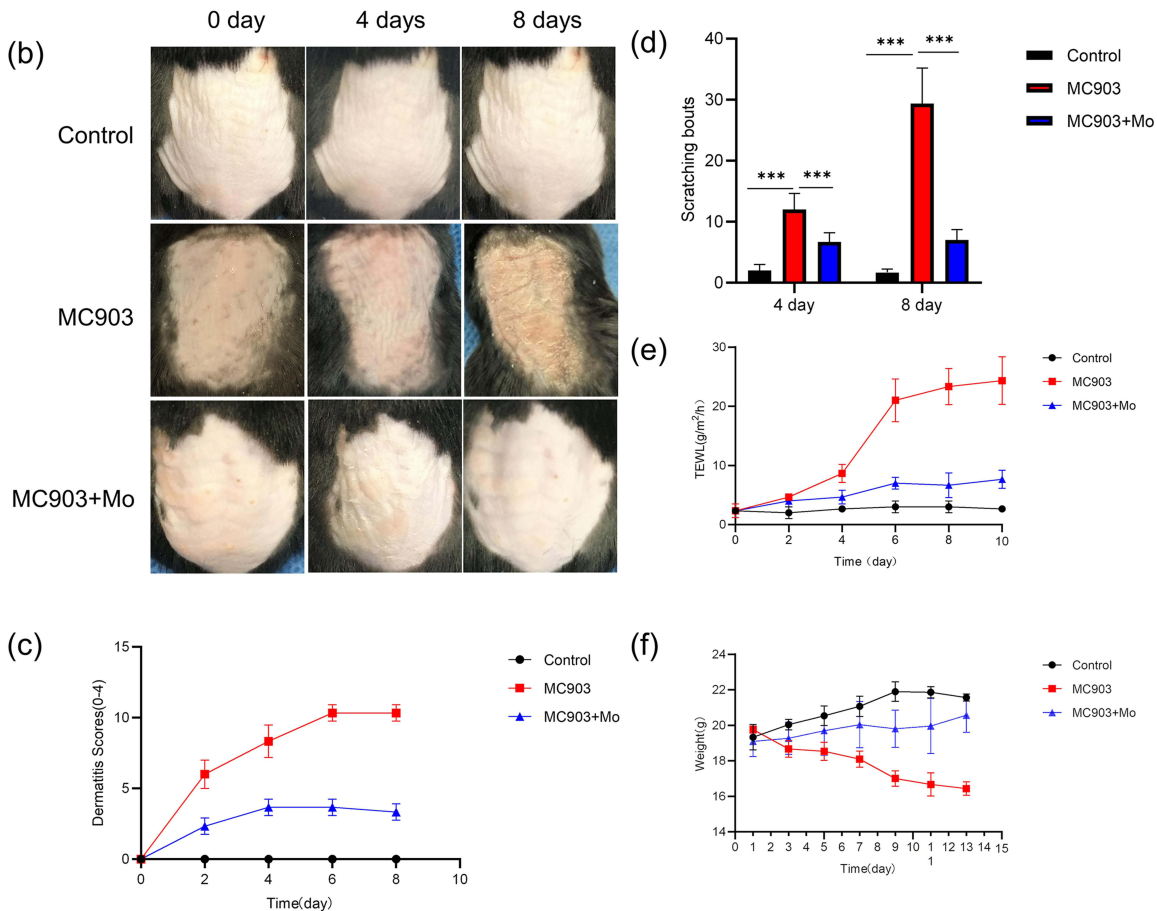
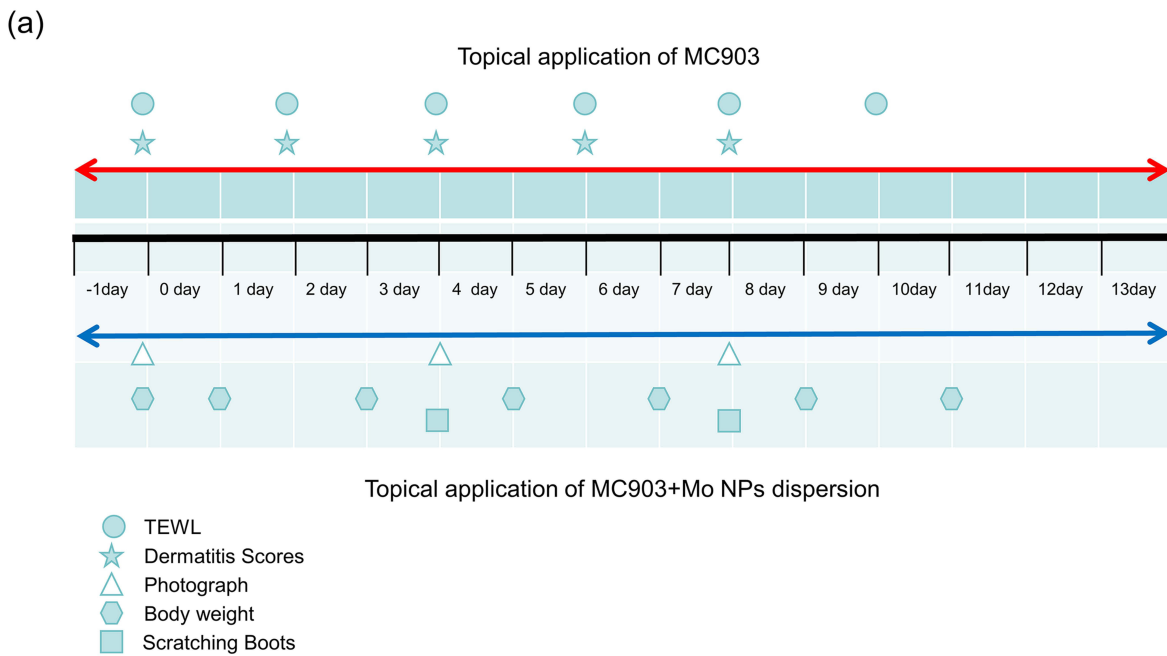


**Figure 4** Favorable therapeutic effects of Mo NPs on AD-like lesions in MC903-induced AD mice. (a) Scheme of the experimental procedure. (b) Typical photographs of dorsal skin lesions of mice in each group. (c) Effects of Mo NPs on dermatitis scores. (d) The number of scratching bouts was calculated on day 4 and 8. (e) TEWL was tested on day 2, 4, 6, 8, and 10. (f) Body weight was measured on day 1, 3, 5, 7, 9, 11 and 13. Results were represented as the mean±SD (n=3). P values were calculated by ANOVA with Tukey's honest significant difference *post-hoc* test (\*\*\*)P < 0.001).

process. Compared to the control group, mice in the AD model group exhibited erythema, edema, and desquamation on the back skin starting from the second day of treatment with MC903, and widespread edema, erythema, and scaling were observed on the dorsal skin accompanied by lichenified changes by the eighth day of MC903 treatment. In contrast, mice treated with topical Mo NPs dispersion showed minimal redness and desquamation on day 4, and no significant aggravation of symptoms was observed by day 13 (Figure 4b). The skin lesion scores of the mice were evaluated on day 0, 2, 4, 6 and 8 and revealed a significant improvement with the application of Mo NPs dispersion. Mo NPs dispersion effectively alleviated AD-like symptoms while decreasing the dermatitis scores of the mice (Figure 4c). Intense itching is also a characteristic manifestation of AD. To assess whether Mo NPs dispersion could improve the itching symptoms in AD mice, we evaluated the scratching behavior of the mice on day 4 and 8. Our findings indicated that topical application of MC903 markedly elevated the frequency of scratching bouts on day 4 and 8. In contrast, the application of Mo NPs dispersion demonstrated a significant reduction in scratching bouts (Figure 4d). To assess the skin barrier function of AD mice, we conducted TEWL tests on the dorsal skin of the mice on day 0, 2, 4, 6, 8, and 10. The results indicated that TEWL gradually increased with the exacerbation of AD skin lesions. MC903-induced mice showed an increase in TEWL versus untreated controls. A reduction in TEWL was observed after treatment with Mo NPs dispersion (Figure 4e). Furthermore, weight measurements on day 1, 3, 5, 7, 9, and 11 indicated a substantial decrease in body weight in AD mice, whereas topical Mo NPs dispersion treatment alleviated the weight loss in MC903-induced mice (Figure 4f).

These findings collectively suggest that topical application of Mo NPs dispersion can significantly improve AD-like skin lesions, alleviate pruritus associated with AD lesions, promote the repair of the compromised skin barrier, reduce TEWL, and ameliorate the weight loss observed in AD mice.

## Mo NPs Ameliorated the Pathological Changes in the Skin Lesions and Inhibited Oxidative Stress in AD Mice

To further investigate the efficacy of Mo NPs on AD, dorsal skin samples from mice were subjected to H&E staining. Figure 5a showed that mice in the MC903 group showed epidermal hyperplasia, hyperkeratosis, spinous layer hypertrophy, and infiltration of inflammatory cells into the dermis, consistent with the pathological features of AD, confirming the successful establishment of a murine model of AD-like disease. Mo NPs markedly alleviated the lesions in the dorsal skin of AD mice. Additionally, the results showed that AD mice had considerably thicker epidermal and dermal skin compared to mice in the control group. However, Mo NPs significantly decreased epidermal and dermal thickness. The IHC results also confirmed that pro-inflammatory marker proteins cyclo-oxygenase-2 (COX2) and inducible nitric oxide synthase (iNOS) were increased significantly in dorsal skin tissues of MC903-induced mice compared with control mice, whereas topical treatment with Mo NPs dispersion resulted in a significant reduction in the expression of COX2 and iNOS in the MC903-induced mice (Figure 5b and c). The expression of TNF- $\alpha$  and TSLP in skin lesions was also studied by IHC, and the results indicated a significant elevation in the expression of TNF- $\alpha$  and TSLP in the MC903 group compared to the control group; this elevation was noticeably mitigated by the administration of Mo NPs dispersion (Figure 5d and e).

## Mo NPs Decreased Expression of AD-Related Cytokines in AD Mice

To further explore the mechanisms by which Mo NPs improved AD-like skin lesions, we conducted PCR testing on dorsal skin lesions to analyze the impact of Mo NPs on the mRNA expression of AD-related factors. As shown in Figure 6a, compared to the control group, the gene expression of pro-inflammatory factors IL-4, IL-13, IL-33, and TSLP in the MC903 group significantly increased. However, topical application of Mo NPs dispersion markedly inhibited the expression of IL-4, IL-13, IL-33, and TSLP. The chemokines associated with AD pathogenesis (MDC, TARC, and RANTES) also exhibited a significant increase in AD mice compared to the control group, and this increase was noticeably attenuated by the administration of Mo NPs dispersion (Figure 6a). PCR was also used to detect the expression of FLG in skin lesions. In the MC903 group, the expression of FLG was significantly decreased compared

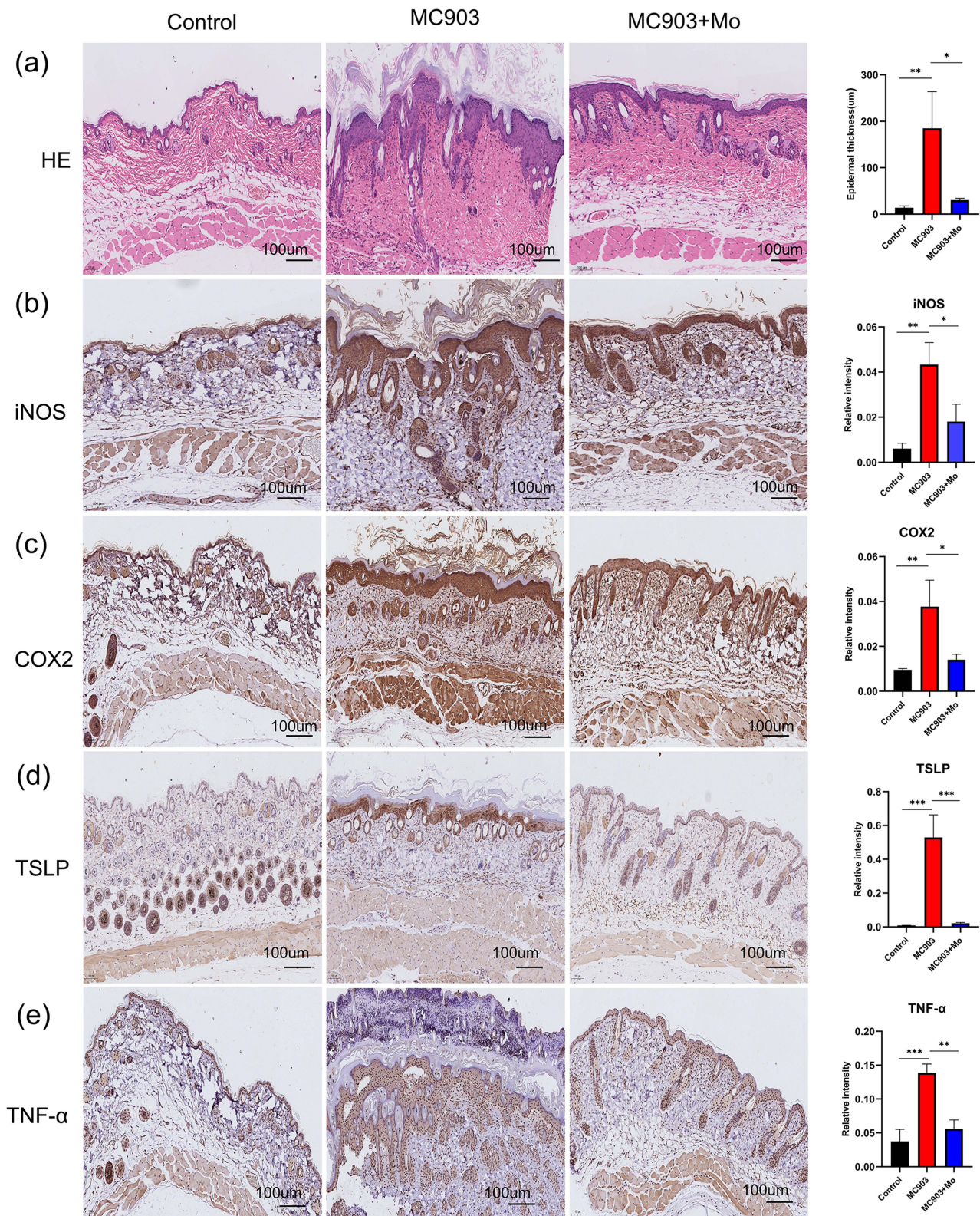


**Figure 5** H&E staining and IHC analysis of the dorsal skin of mice in each group. **(a)** Histological features were analyzed by H&E staining. **(b–e)** iNOS, COX2, TSLP and TNF- $\alpha$  IHC staining in the tissue sections of different groups. Data were presented as mean  $\pm$  SD from three independent replicates, and P values were calculated by ANOVA with Tukey's honest significant difference *post-hoc* test (\* $P < 0.1$ , \*\* $P < 0.01$ , and \*\*\* $P < 0.001$ ).

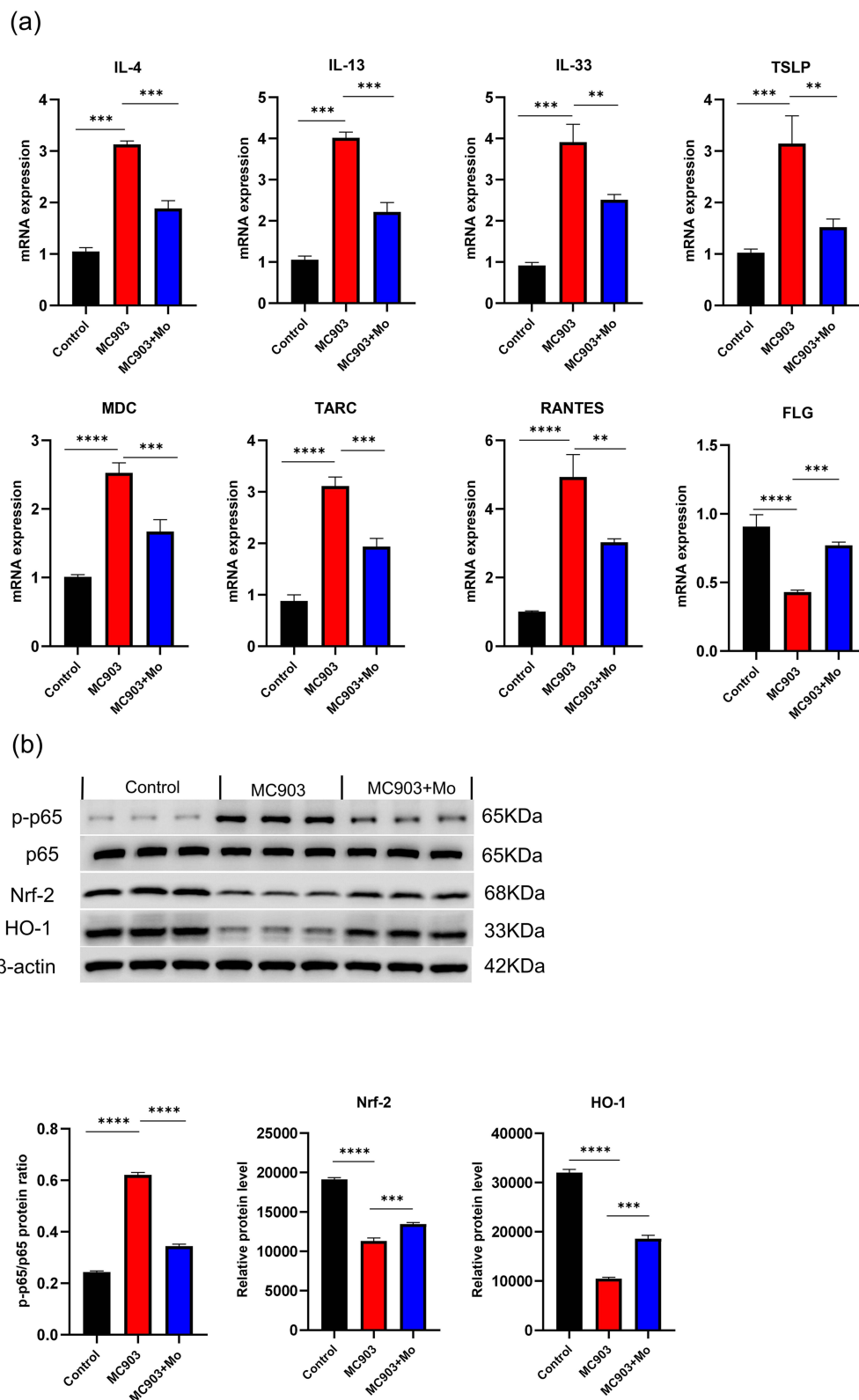


**Figure 6** Therapeutic mechanisms of Mo NPs on MC903-induced AD mice. (a) Skin mRNA levels of pro-inflammatory cytokines IL-4, IL-13, IL-33, TSLP, chemokines (MDC, TARC and RANTES), and FLG. (b) Western blot analysis of the expression of p-P65, P65 and Nrf2/HO-1 in the dorsal skin of mice in each group. Data were presented as mean  $\pm$  SD from three independent replicates, and P values were calculated by one-way ANOVA with Tukey's honest significant difference post-hoc test (\*\*P < 0.01, \*\*\*P < 0.001, and \*\*\*\*P < 0.0001).

with the control group (Figure 6a). Meanwhile, the expression of FLG in mice treated with Mo NPs dispersion was significantly increased compared with that in MC903-induced mice.

The above results indicated that the topical application of Mo NPs dispersion notably suppressed the gene expression of pro-inflammatory factors IL-4, IL-13, IL-33, and TSLP, as well as chemokines MDC, TARC, and RANTES, but increased the expression of FLG in the skin of AD-like mice that promoted the repair of the compromised skin barrier and reduced TEWL.

## Mo NPs Promoted the Expression of Nrf2/HO-1 by Inhibiting the NF- $\kappa$ B Signaling Pathway

Nrf2, and HO-1 protein levels and NF- $\kappa$ B P65 phosphorylation levels in mice dermal tissue were quantified by Western blotting (Figure 6b). Compared to the control group, there was a significant increase of p-P65 levels in the skin lesions of MC903-induced mice, indicating excessive phosphorylation of P65 and activation of the NF- $\kappa$ B signaling pathway. The protein expression of Nrf2 and HO-1 was noticeably suppressed. Consistent with these *in vitro* results, a topical application of Mo NPs dispersion could inhibit the phosphorylation of P65 and promote the expression of Nrf2 and HO-1 in the skin lesions of MC903-induced mice. These results suggested that Mo NPs dispersion could inhibit excessive P65 phosphorylation, suppress the overactivation of the NF- $\kappa$ B signaling pathway, promote the expression of Nrf2 and HO-1, reduce the secretion of COX2 and iNOS, and inhibit oxidative stress reactions in skin lesions of AD-like mice, thereby ameliorating the skin lesions.

## Discussion

Currently, the treatment for AD involves topical application of corticosteroids and calcineurin inhibitors.<sup>41</sup> In recent years, biological agents and janus kinase inhibitors have provided additional options for AD treatment. However, the high cost and potential long-term side effects have made it difficult for some patients to choose these medications.<sup>42</sup> Therefore, there is an urgent need to develop more effective and convenient drugs for treating AD.

Oxidative stress plays a significant role in the onset of AD, and Mo NPs, as an essential trace element in the human body, exhibit excellent antioxidant properties. As a result, we planned to use a prepared Mo NPs dispersion for topical treatment of AD. Our results indicated that topical application of Mo NPs dispersion had a positive therapeutic effect on MC903-induced skin lesions in mice. Diffuse erythema, thickened patches, significant desquamation, and crusting were observed on the dorsal skin of mice treated with MC903 alone. Topical application of Mo NPs dispersion significantly alleviated the MC903-induced symptoms in mice, reducing the severity and affected area of erythema, macules, edema, and desquamation. Dermatitis scores also showed a noticeable decrease. Simultaneously, itching was significantly relieved and TEWL was notably reduced in AD mice. Histological examination with H&E staining revealed that topical application of Mo NPs dispersion significantly reduced epidermal thickening and improved the pathological features of hyperkeratosis and sphenoid layer hypertrophy. We also found that topical application of Mo NPs dispersion could promote the expression of the FLG gene. FLG is a crucial protein related to skin barrier function, and in the skin lesions of AD patients, there is often a decrease in FLG expression that is a major factor in the compromised skin barrier of AD patients.<sup>43</sup> Therefore, we speculate that promoting FLG expression is one of the mechanisms by which topical Mo NPs dispersion repairs skin barrier function. Mo NPs dispersion also inhibited the expression of TSLP, inflammatory factors (IL-4, IL-13, IL-33) and chemokines (MDC, TARC, RANTES). TSLP, Th2 cytokines and chemokines play crucial roles in the pathogenesis of AD. Mo NPs inhibit skin inflammation by suppressing the excessive expression of these factors. Mo NPs could further inhibit the expression of key oxidative stress factors, namely COX2 and iNOS, in skin lesions of AD mouse. Both cell culture and animal experiments have confirmed the excellent antioxidant effect of Mo NPs. Further studies confirmed that Mo NPs could inhibit the excessive phosphorylation of the NF- $\kappa$ B pathway in keratinocytes and in the skin lesions of MC903-induced mice, thereby suppressing the overactivation of the NF- $\kappa$ B pathway. Excessive activation of the NF- $\kappa$ B pathway promotes the secretion of various pro-inflammatory factors.<sup>44</sup> Conversely, Mo NPs could promote the activation of the Nrf2/HO-1 signaling pathway. Nrf2 and HO-1 are crucial proteins involved in antioxidant defense. The Nrf2/HO-1 signaling pathway plays an important role in maintaining redox homeostasis by activating the expression of genes encoding antioxidant-related proteins<sup>45</sup> that in

turn inhibits the generation of ROS.<sup>39</sup> Nrf2 plays a pivotal role in regulating antioxidant proteins, including HO-1.<sup>46</sup> HO-1 attenuates the development of AD-like lesions in mice.<sup>47</sup> Nrf2 and NF- $\kappa$ B signaling pathways interact through multiple mechanisms. Excessive activation of the NF- $\kappa$ B pathway inhibits Nrf2, thereby suppressing the expression of downstream genes with cellular protective functions.<sup>48,49</sup> The NF- $\kappa$ B pathway can also promote the expression of inflammatory factors, including COX2 and TNF- $\alpha$ .<sup>44</sup> Additionally, Nrf2 and HO-1 can inhibit the activation of the NF- $\kappa$ B pathway.<sup>50</sup> Based on the above research results, we have summarized the possible mechanisms of using Mo NPs for the topical treatment of atopic dermatitis with a schematic diagram (Figure 7). We speculate that Mo NPs inhibit excessive activation of the NF- $\kappa$ B pathway, promote the expression of Nrf2 and HO-1 proteins, and suppress the expression of COX2 and iNOS, thereby suppressing oxidative stress. The inhibition of oxidative stress can reduce the secretion and expression of TSLP, inflammatory factors, and chemokines. These, in turn, can reduce further damage to the epidermis and dermis, thereby repairing the impaired skin barrier. The restored skin barrier can reduce TEWL, alleviate skin inflammation, and oxidative stress, creating a positive cycle that improves AD skin lesions.

Our team has conducted extensive research and exploration on the use of Mo NPs in the treatment of skin diseases.<sup>20,21,51</sup> Recently, a study on the treatment of psoriasis with Mo NPs has been published.<sup>51</sup> Compared to previous studies, this research delves deeper into the mechanisms of Mo NPs in combating oxidative stress. It was discovered that Mo NPs affects the interaction between the NF- $\kappa$ B signaling pathway and the Nrf2/HO-1 signaling pathways. Additionally, it was confirmed that Mo NPs influences the expression of the skin barrier-related protein FLG. Psoriasis is characterized by Th1-type inflammation, whereas AD is Th2-type inflammation. This study also found that Mo NPs significantly inhibits Th2-type cytokines and chemokines. One limitation of our study is that the study focused primarily on biochemical markers and histopathological changes. Future research could benefit from exploring additional molecular mechanisms underlying the observed effects.

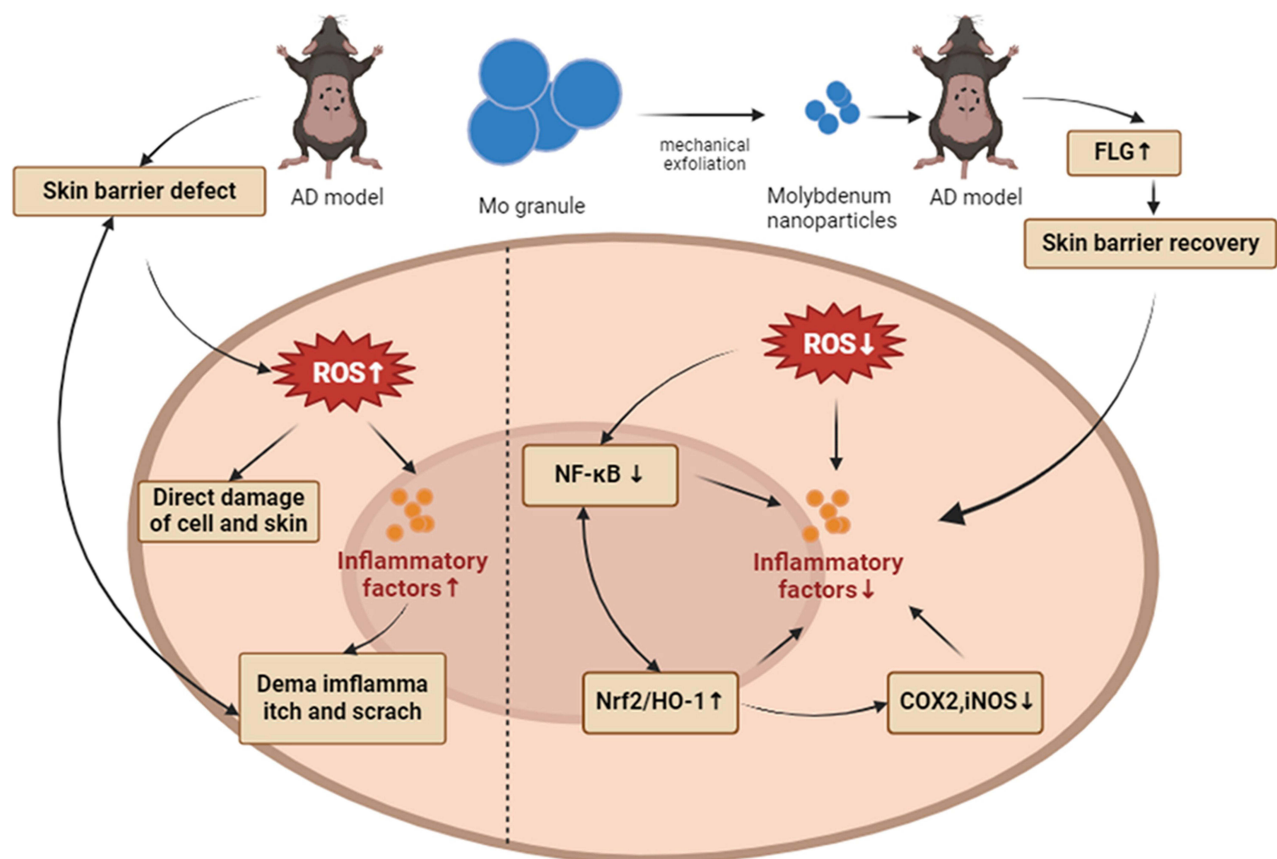


**Figure 7** Schematic showing Mo NPs used in the treatment of MC903-induced atopic dermatitis-like symptoms. Mo NPs inhibited oxidative stress reactions by inhibiting NF- $\kappa$ B pathway and activating Nrf2 /HO-1 pathway. Mo NPs could also repair the skin barrier by promoting FLG expression.

## Conclusions

Topical application of Mo NPs has a significant therapeutic effect on AD skin lesions. Our results demonstrated that the topical application of Mo NPs dispersion markedly reduced the severity of skin lesions, relieved itching, repaired the skin barrier, suppressed the weight loss of AD mice, and ameliorated the pathological changes in AD skin lesions. The primary mechanism may involve inhibiting the excessive activation of the NF- $\kappa$ B pathway, promoting the expression of Nrf2 and HO-1 proteins, suppressing the expression of COX2 and iNOS, and inhibiting oxidative stress reactions. Additionally, Mo NPs inhibited the expression of TSLP, inflammatory factors (IL-4, IL-13, IL-33), chemokines (MDC, TARC, RANTES), and reduced skin inflammation. Lastly, they promoted the expression of FLG, further repairing the skin barrier. Therefore, Mo NPs could address three pivotal mechanisms in the pathogenesis of AD concurrently, and their topical application showed no discernible toxic side effects. We speculate that Mo NPs have great potential as a topical treatment for AD, and further exploration is needed to fully understand their mechanism of action in the treatment of AD.

## Abbreviations

AD, atopic dermatitis; COX2, cyclo-oxygenase-2; DCFH-DA, 2,7-dichlorodihydrofluorescein diacetate; FLG, filaggrin; HO-1, heme oxygenase-1; IL, interleukins; iNOS, inducible nitric oxide synthase; MDC, macrophage derived chemokine; Mo NPs, molybdenum nanoparticles; NF- $\kappa$ B, nuclear factor kappa-B; Nrf2, nuclear factor erythroid 2-related factor 2; RANTES, regulated on activation normal T cell express and secreted; ROS, reactive oxygen species; TARC, thymic and activating regulatory chemokine; TEM, transmission electron microscopy; TEWL, transepidermal water loss; TNF- $\alpha$ , tumor necrosis factor- $\alpha$ ; TSLP, thymic stromal lymphopoietin; XPS, X-ray photoelectron spectroscopy; XRD, X-ray diffraction.

## Data Sharing Statement

The data are available from the corresponding author on reasonable request.

## Ethics Approval and Consent to Participate

The Institutional Animal Care and Use Committee of the Experimental Animal Welfare and Ethics Management Committee of Tongji University (Laboratory animal licences 2020-002, Shanghai, China) approved all animal experiments. All experimental protocols followed Tongji University Guidelines for Ethical Review of Laboratory Animal Welfare. Consent to participate was not applicable.

## Acknowledgments

This work was supported, in part, by the National Natural Science Foundation of China (82202018), the Jiangxi Provincial Health Commission Project (SKJP220203555), the Pudong New District Health and Family Planning Commission (PWZzb2022-19), and the Fundamental Research Funds for the Central Universities (22120240377).

## Funding

National Natural Science Foundation of China 82202018; Jiangxi Provincial Health Commission Project (SKJP220203555); Pudong New District Health and Family Planning Commission (PWZzb2022-19); Fundamental Research Funds for the Central Universities (22120240377).

## Disclosure

The authors declare no conflicts of interest in this work.

## References

1. Schuler CF, Billi AC, Maverakis E, Tsoi LC, Gudjonsson JE. Novel insights into atopic dermatitis. *J Allergy Clin Immunol.* 2023;151:1145–1154. doi:10.1016/j.jaci.2022.10.023
2. Laughter MR, Maymone MBC, Mashayekhi S, et al. The global burden of atopic dermatitis: lessons from the global burden of disease study 1990–2017. *Br J Dermatol.* 2021;184:304–309. doi:10.1111/bjd.19580



3. Drislane C, Irvine AD. The role of filaggrin in atopic dermatitis and allergic disease. *Ann Allergy Asthma Immunol.* 2020;124:36–43. doi:10.1016/j.anai.2019.10.008
4. Bertino L, Guarneri F, Cannavo SP, Casciaro M, Pioggia G, Gangemi S. Oxidative stress and atopic dermatitis. *Antioxidants.* 2020;9(3):196. doi:10.3390/antiox9030196
5. Liu Z, Fan Z, Liu J, et al. Melittin-carrying nanoparticle suppress T cell-driven immunity in a murine allergic dermatitis model. *Adv Sci.* 2023;10:e2204184.
6. Borgia F, Custurone P, Peterle L, Pioggia G, Gangemi S. Role of epithelium-derived cytokines in atopic dermatitis and psoriasis: evidence and therapeutic perspectives. *Biomolecules.* 2021;11(12):1843.
7. Wu Y, Zhou Z, Zhang M, Li S, Sun M, Song Z. Hollow manganese dioxide-chitosan hydrogel for the treatment of atopic dermatitis through inflammation-suppression and ROS scavenging. *J Nanobiotechnology.* 2023;21:432. doi:10.1186/s12951-023-02174-w
8. Choi JK, Park JY, Lee S, et al. Greater plasma protein adsorption on mesoporous silica nanoparticles aggravates atopic dermatitis. *Int J Nanomed.* 2022;17:4599–4617. doi:10.2147/IJN.S383324
9. Ni Q, Zhang P, Li Q, Han Z. Oxidative stress and gut microbiome in inflammatory skin diseases. *Front Cell Dev Biol.* 2022;10:849985. doi:10.3389/fcell.2022.849985
10. Wang P, Hu G, Zhao W, et al. Continuous ZnO nanoparticle exposure induces melanoma-like skin lesions in epidermal barrier dysfunction model mice through anti-apoptotic effects mediated by the oxidative stress-activated NF- $\kappa$ B pathway. *J Nanobiotechnology.* 2022;20:111. doi:10.1186/s12951-022-01308-w
11. Borgia F, Li Pomi F, Vaccaro M, et al. Oxidative stress and phototherapy in atopic dermatitis: mechanisms, role, and future perspectives. *Biomolecules.* 2022;12(12):1904.
12. Zhou Q, Xue S, Zhang L, Chen G. Trace elements and the thyroid. *Front Endocrinol.* 2022;13:904889. doi:10.3389/fendo.2022.904889
13. Sardesai VM. Molybdenum: an essential trace element. *Nutr Clin Pract.* 1993;8:277–281. doi:10.1177/0115426593008006277
14. Schroeder HA, Balassa JJ, Tipton IH. Essential Trace Metals in Man: Molybdenum. *J Chronic Dis.* 1970;23:481–499. doi:10.1016/0021-9681(70)90056-1
15. Keck CM, Anantaworasakul P, Patel M, et al. A new concept for the treatment of atopic dermatitis: silver-nanolipid complex (sNLC). *Int J Pharm.* 2014;462:44–51. doi:10.1016/j.ijpharm.2013.12.044
16. Zhao K, Pu S, Sun L, Zhou D. Gentiopicroside-loaded chitosan nanoparticles inhibit TNF- $\alpha$ -induced proliferation and inflammatory response in HaCaT keratinocytes and ameliorate imiquimod-induced dermatitis lesions in mice. *Int J Nanomed.* 2023;18:3781–3800. doi:10.2147/IJN.S406649
17. Li M, Chen B, Xu L, et al. Topical bismuth oxide-manganese composite nanospheres alleviate atopic dermatitis-like inflammation. *J Nanobiotechnology.* 2023;21:430. doi:10.1186/s12951-023-02207-4
18. Qiu L, Ouyang C, Zhang W, et al. Zn-MOF hydrogel: regulation of ROS-mediated inflammatory microenvironment for treatment of atopic dermatitis. *J Nanobiotechnology.* 2023;21:163. doi:10.1186/s12951-023-01924-0
19. Xu J, Cai R, Zhang Y, Mu X. Molybdenum disulfide-based materials with enzyme-like characteristics for biological applications. *Colloids Surf B Biointerfaces.* 2021;200:111575. doi:10.1016/j.colsurfb.2021.111575
20. Xiao Q, Lu Y, Yao W, et al. Molybdenum nanoparticles as a potential topical medication for alopecia treatment through antioxidant pathways that differ from minoxidil. *J Trace Elem Med Biol.* 2024;82:127368. doi:10.1016/j.jtmb.2023.127368
21. Lu Y, Jia C, Gong C, et al. A hydrogel system containing molybdenum-based nanomaterials for wound healing. *Nano Res.* 2023;16:5368–5375. doi:10.1007/s12274-022-5255-9
22. Wang J, Sui L, Huang J, et al. MoS<sub>2</sub>-based nanocomposites for cancer diagnosis and therapy. *Bioact Mater.* 2021;6:4209–4242. doi:10.1016/j.bioactmat.2021.04.021
23. Huang J, Deng G, Wang S, et al. A NIR-II Photoactivatable "ROS Bomb" with High-Density Cu(2) O-Supported MoS<sub>2</sub> nanoflowers for anticancer therapy. *Adv Sci.* 2023;10:e2302208.
24. Zhang C, Wang H, Yang X, et al. Oral zero-valent-molybdenum nanodots for inflammatory bowel disease therapy. *Sci Adv.* 2022;8:eabp9882.
25. Centa UG, Kocbez A, Kapin SD, Remkar M. Polymer blend containing MoO<sub>3</sub> nanowires with antibacterial activity against staphylococcus epidermidis ATCC 12228. *J Nanomater.* 2020;2007:1.
26. Centa UG, Sternisa M, Visic B, Federl Z, Mozina SS, Remskar M. Novel nanostructured and antimicrobial PVDF-HFP/PVP/MoO<sub>3</sub> composite. *Surface Innovations.* 2021;9:1.
27. Saheb Kashaf S, Harkins CP, Deming C, et al. Staphylococcal diversity in atopic dermatitis from an individual to a global scale. *Cell Host Microbe.* 2023;31:578–592.e576. doi:10.1016/j.chom.2023.03.010
28. Gao JF, Tang L, Luo F, et al. Nicotinamide mononucleotide ameliorates DNFB-induced atopic dermatitis-like symptoms in mice by blocking activation of ROS-mediated JAK2/STAT5 signaling pathway. *Int Immunopharmacol.* 2022;109:108812. doi:10.1016/j.intimp.2022.108812
29. Koerdt S, Tanner N, Rommel N, et al. An Immunohistochemical Study on the Role of Oxidative and Nitrosative Stress in Irradiated Skin. *Cells Tissues Organs.* 2017;203:12–19. doi:10.1159/000447584
30. Dubray F, Moldovan S, Kouvas C, et al. Direct Evidence for Single Molybdenum Atoms Incorporated in the Framework of MFI Zeolite Nanocrystals. *J Am Chem Soc.* 2019;141:8689–8693. doi:10.1021/jacs.9b02589
31. Simonetti O, Bacchetti T, Ferretti G, et al. Oxidative stress and alterations of paraoxonases in atopic dermatitis. *Antioxidants.* 2021;10(5):697.
32. Leung DY, Bieber T. Atopic dermatitis. *Lancet.* 2003;361:151–160. doi:10.1016/S0140-6736(03)12193-9
33. Das P, Mounika P, Yellurkar ML, et al. Keratinocytes: an enigmatic factor in atopic dermatitis. *Cells.* 2022;11(10):1683.
34. Mehta NN, Teague HL, Swindell WR, et al. IFN- $\gamma$  and TNF- $\alpha$  synergism may provide a link between psoriasis and inflammatory atherogenesis. *Sci Rep.* 2017;7:13831. doi:10.1038/s41598-017-14365-1
35. Klonowska J, Gleń J, Trzeciak M, Nowicki R. Combination of FLG mutations and SNPs of IL-17A and IL-19 influence on atopic dermatitis occurrence. *Postepy Dermatol Alergol.* 2022;39:200–208. doi:10.5114/ada.2021.105412
36. Vestergaard C, Bang K, Gesser B, Yoneyama H, Matsushima K, Larsen CG. A Th2 chemokine, TARC, produced by keratinocytes may recruit CLA<sup>+</sup>CCR4<sup>+</sup> lymphocytes into lesional atopic dermatitis skin. *J Invest Dermatol.* 2000;115:640–646. doi:10.1046/j.1523-1747.2000.00115.x
37. Tang F, Ma X, Sun J, et al. Cell-penetrating heme oxygenase-1 in the therapy of atopic dermatitis in mice. *Exp Ther Med.* 2021;22:941. doi:10.3892/etm.2021.10373

38. Choi JH, Jin SW, Han EH, et al. Platycodon grandiflorum root-derived saponins attenuate atopic dermatitis-like skin lesions via suppression of NF- $\kappa$ B and STAT1 and activation of Nrf2/ARE-mediated heme oxygenase-1. *Phytomedicine*. 2014;21:1053–1061. doi:10.1016/j.phymed.2014.04.011
39. Rahman MS, Alam MB, Kim YK, et al. Activation of Nrf2/HO-1 by Peptide YD1 Attenuates Inflammatory Symptoms through Suppression of TLR4/MYD88/NF- $\kappa$ B Signaling Cascade. *Int J Mol Sci*. 2021;22(10):5161.
40. Ogawa T, Ishitsuka Y. The Role of KEAP1-NRF2 System in Atopic Dermatitis and Psoriasis. *Antioxidants*. 2022;11(7):1397. doi:10.3390/antiox11071397
41. Werfel T, Heratizadeh A, Aberer W, et al. S3 guideline atopic dermatitis: part 1 - General aspects, topical and non-drug therapies, special patient groups. *J Dtsch Dermatol Ges*. 2024;22:137–153. doi:10.1111/ddg.15230
42. Langan SM, Irvine AD, Weidinger S. Atopic dermatitis. *Lancet*. 2020;396:345–360. doi:10.1016/S0140-6736(20)31286-1
43. Moosbrugger-Martinz V, Leprince C, Méchin MC, et al. Revisiting the roles of filaggrin in atopic dermatitis. *Int J Mol Sci*. 2022;23(10):5318.
44. Zhang Q, Lenardo MJ, Baltimore D. 30 Years of NF- $\kappa$ B: a blossoming of relevance to human pathobiology. *Cell*. 2017;168:37–57. doi:10.1016/j.cell.2016.12.012
45. Jin W, Botchway BOA, Liu X. Curcumin can activate the Nrf2/HO-1 signaling pathway and scavenge free radicals in spinal cord injury treatment. *Neurorehabil Neural Repair*. 2021;35:576–584. doi:10.1177/15459683211011232
46. Loboda A, Damulewicz M, Pyza E, Jozkowicz A, Dulak J. Role of Nrf2/HO-1 system in development, oxidative stress response and diseases: an evolutionarily conserved mechanism. *Cell Mol Life Sci*. 2016;73:3221–3247. doi:10.1007/s00018-016-2223-0
47. Kirino M, Kirino Y, Takeno M, et al. Heme oxygenase 1 attenuates the development of atopic dermatitis-like lesions in mice: implications for human disease. *J Allergy Clin Immunol*. 2008;122:290–297. doi:10.1016/j.jaci.2008.05.031
48. Yu M, Li H, Liu Q, et al. Nuclear factor p65 interacts with Keap1 to repress the Nrf2-ARE pathway. *Cell Signal*. 2011;23:883–892. doi:10.1016/j.cellsig.2011.01.014
49. Helou DG, Martin SF, Pallardy M, Chollet-Martin S, Kerdine-Römer S. Nrf2 involvement in chemical-induced skin innate immunity. *Front Immunol*. 2019;10:1004. doi:10.3389/fimmu.2019.01004
50. Wardyn JD, Ponsford AH, Sanderson CM. Dissecting molecular cross-talk between Nrf2 and NF- $\kappa$ B response pathways. *Biochem Soc Trans*. 2015;43:621–626. doi:10.1042/BST20150014
51. Guo J, Xiao Q, Lu Y, et al. Molybdenum nanoparticles ameliorate psoriatic lesions by inhibiting the ROS/NF- $\kappa$ B Signaling Axis. *ACS Appl Nano Mater*. 2024;7(11):12839–12847. doi:10.1021/acsanm.4c01363

International Journal of Nanomedicine

Dovepress

## Publish your work in this journal

The International Journal of Nanomedicine is an international, peer-reviewed journal focusing on the application of nanotechnology in diagnostics, therapeutics, and drug delivery systems throughout the biomedical field. This journal is indexed on PubMed Central, MedLine, CAS, SciSearch<sup>®</sup>, Current Contents<sup>®</sup>/Clinical Medicine, Journal Citation Reports/Science Edition, EMBase, Scopus and the Elsevier Bibliographic databases. The manuscript management system is completely online and includes a very quick and fair peer-review system, which is all easy to use. Visit <http://www.dovepress.com/testimonials.php> to read real quotes from published authors.

Submit your manuscript here: <https://www.dovepress.com/international-journal-of-nanomedicine-journal>